Adsorption 11: 391–396, 2005

Effect of Confinement on Freezing of CCl_4 in Cylindrical Pores

MALGORZATA SLIWINSKA-BARTKOWIAK
Institute of Physics, Adam Mickiewicz University, Umultowska 85, 61-614 Poznan, Poland

FRANCISCO R. HUNG,* ERIK E. SANTISO AND BENOIT COASNE
Department of Chemical and Biomolecular Engineering, North Carolina State University, Raleigh, NC 27606-7905, USA
frhung@unity.ncsu.edu

GRAZYNA DUDZIAK
Institute of Physics, Adam Mickiewicz University, Umultowska 85, 61-614 Poznan, Poland

FLOR R. SIPERSTEIN
Departament d'Enginyeria Química, Universitat Rovira i Virgili, Campus Sescelades, Av. dels Països Catalans 26, 43007, Tarragona, Spain

KEITH E. GUBBINS
Department of Chemical and Biomolecular Engineering, North Carolina State University, Raleigh, NC 27606-7905, USA

Abstract. We report experimental and molecular simulation results on the freezing and melting of fluids confined within cylindrical pores. Dielectric relaxation spectroscopy was used to determine the experimental melting points of carbon tetrachloride confined within multi-walled carbon nanotubes. Molecular simulations in the grand canonical ensemble and free energy calculations were performed for the same system to determine the structure and thermodynamic stability of the confined phases, as well as the temperatures and the order of the phase transitions. Both simulations and experiments show evidence of a rich phase behavior in confinement, with a number of inhomogeneous phases that are stable over extended temperature ranges. Multiple transition temperatures both above and below the bulk melting point were obtained from experiments and simulations, with good agreement between both series of results.

Keywords: confinement, solid-fluid transitions, molecular simulation, dielectric relaxation, carbon nanotubes

1. Introduction

Recent studies have shown a rich phase behavior associated with freezing of host phases in porous materials (for a review see Gelb et al., 1999). Depending on the adsorbate and the porous material, the freezing temperature may be lowered or raised compared to the bulk value, and new surface-driven phases may intervene between the liquid and solid phases in the pore. Recently, it has been shown (Radhakrishnan et al., 2002a, and references therein) that the phase behavior of pure substances in confinement depends on the pore size and shape, and on the ratio of the adsorbate-wall to adsorbate-adsorbate interactions.

---

*To whom correspondence should be addressed.

In a previous study (Hung et al., 2004) we presented experimental and simulation results for freezing and melting of fluids, such as nitrobenzene and carbon tetrachloride, confined within multi-walled carbon nanotubes (MWCNT). Results from dielectric relaxation spectroscopy and parallel tempering Monte Carlo suggested the existence of several inhomogeneous phases, and provided information about the multiple transition temperatures found in confinement. Although the use of the parallel tempering technique in simulations greatly reduces the probability of getting trapped in a metastable state, a free energy calculation is required to rigorously determine the thermodynamic stability of each phase, as well as to unambiguously establish the values of the thermodynamic transition temperatures. A brief summary of the results of our free energy calculations for CCl_4 within MWCNT is presented in this work, which forms part of a larger study involving experiments and simulations of freezing and melting within cylindrical pores. The simulation results presented here provide evidence of a rich phase behavior in confinement, which is confirmed by our experiments using dielectric relaxation spectroscopy.

2. Experimental and Simulation Methods

The MWCNT used in our experiments were synthesized at CNRS-Orléans *via* a catalytic decomposition of acetylene at 600°C on a $Co_xMg_{(1-x)}O$ solid solution (Delpeux et al., 2002). The MWCNT samples were purified using concentrated HCl, and some of them were oxidized by a treatment with CO_2 to open the nanotube tips. Scanning and transmission electron microscopy (SEM/TEM), and nitrogen adsorption measurements showed that the MWCNT had seven molecular layers and a narrow pore size distribution, with average internal and external diameters of 5 and 10 nm. The carbon tetrachloride samples were reagent grade chemicals, and were distilled twice at reduced pressure before their use in experiments. The conductivity of the purified CCl_4 samples was found to be less than $10^{-16}\ \Omega^{-1}\ m^{-1}$. The MWCNT were kept under vacuum (10^{-3} torr) prior to and during the introduction of the fluid samples; in addition, the MWCNT were heated to 120°C to remove traces of air and moisture. Dielectric relaxation spectroscopy was used to determine the experimental melting points of confined CCl_4. The capacitance C of the parallel plate capacitor filled with the sample was measured at different temperatures T and frequencies ω using a Solartron 1260 gain impedance analyzer. As a solid phase sample is heated, phase transitions such as melting manifest themselves by changes in the C *vs.* T behavior. For the case of confined CCl_4, the sample was introduced between the capacitor plates as a suspension of CCl_4-filled MWCNT in the pure fluid. Further details of these experimental methods are described elsewhere (Sliwinska-Bartkowiak et al., 1999; Hung et al., 2004).

In our simulations, CCl_4 was described as a Lennard-Jones (LJ) particle, with parameters fitted (Radhakrishnan et al., 2002a) to the freezing point and liquid density at bulk coexistence: $\sigma_{ff} = 0.514$ nm, $\varepsilon_{ff}/k_B = 366.1$ K. Nevertheless, the correct bulk crystal structure is not predicted: real CCl_4 forms a rhombohedral (Ib) phase at 250 K and a monoclinic (II) phase at 225 K (Domalski and Hearing, 2003), whereas LJ CCl_4 solidifies into an fcc crystal. As a result, properties such as latent heat of melting will not be correctly predicted, but our model will be good enough to compare the transition temperatures found from experiments and simulations. The carbon nanotube was modeled as a structureless, cylindrical pore of diameter $D = 5$ nm and length $L = 30.84$ nm, surrounded by a semi-infinite solid (Peterson et al., 1986), with parameters equal to those of graphite: $\rho_w = 114\ \text{nm}^{-3}$, $\sigma_{ww} = 0.340$ nm and $\varepsilon_{ww}/k_B = 28.0$ K. Our Monte Carlo simulations were performed in the grand canonical ensemble, and included parallel tempering (Yan and de Pablo, 1999), and the Landau free energy method (Radhakrishnan and Trout, 2002). Since strong layering is observed in the system, a representative quasi-two-dimensional configuration of the molecules within a layer j can be obtained by cutting the layer along the axial direction z and unrolling it flat. To study the freezing behavior of the molecular layer j, we monitored the in-plane positional pair correlation function $g_j(r)$ (where r is the in-layer distance), given by the radial distribution function measured within the unwrapped layer j. We also measured the in-plane, bond orientational pair correlation function $G_{6,j}(r)$, and the 2-D bond orientational order parameters $\Phi_{6,j}$ (Nelson and Halperin, 1979):

$$\begin{aligned} G_{6,j}(r) &= \langle \Psi^*_{6,j}(0)\Psi_{6,j}(r)\rangle; \\ \Psi_{6,j}(\mathbf{r}) &= \frac{1}{N_b}\sum_{k=1}^{N_b}\exp(i6\theta_k); \qquad (1) \\ \Phi_{6,j} &= \langle |\Psi_{6,j}(\mathbf{r})| \rangle \end{aligned}$$

where N_b is the number of nearest neighbor bonds and θ_k is the orientation of the nearest neighbor bond k

with respect to an arbitrary axis. These pair correlation functions and bond order parameters were monitored for all the adsorbate layers with the exception of the two innermost molecular layers, for which we measured the 3-D radial distribution function $g(R)$ (where R is the 3-D distance between molecules), corrected by excluded volume effects (Morineau and Alba-Simionesco, 2003); and the 3-D bond order parameter Q_6 (Steinhardt et al., 1983):

$$\begin{aligned} Q_l &= \left[\frac{4\pi}{2l+1}\sum_{m=-l}^{l}|\bar{Q}_{lm}|^2\right]^{1/2}; \\ \bar{Q}_{lm} &= \frac{1}{N_b}\sum_{i=1}^{N_b} Y_{lm}(\theta_i, \varphi_i) \end{aligned} \tag{2}$$

where $l = 6$ and Y_{lm} are spherical harmonics. We determined the Landau free energy Λ of the confined phases as a function of the previous bond order parameters. For our system, the Landau free energies were obtained from:

$$\begin{aligned} \Lambda = &-k_B T \ln[P(\Phi_{6,\text{contact}}; \Phi_{6,\text{second}}; \Phi_{6,\text{third}}; Q_{6,\text{inner}})] \\ &+ \text{constant} \end{aligned} \tag{3}$$

The probability distribution function P is determined by collecting statistics of the number of occurrences of simultaneous values of these order parameters in a four-dimensional histogram. Further details of the simulation methods used in this work are given elsewhere (Yan and de Pablo, 1999; Radhakrishnan et al., 2002a; Radhakrishnan and Trout, 2002; Hung et al., 2004).

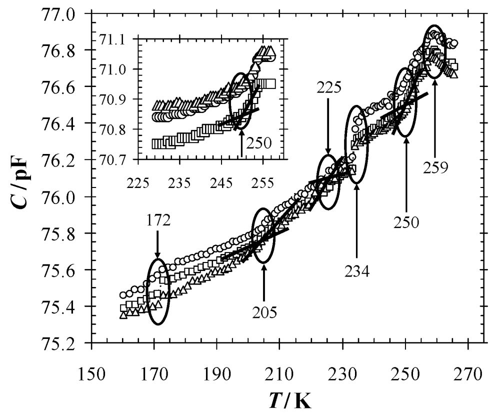

Figure 1. Capacitance C as a function of temperature T for CCl_4 adsorbed on closed (inset) and open-tip MWCNT, with average internal and external pore diameters of 5 nm and 10 nm. The measurements were performed at frequencies ω equal to 30 kHz (circles), 100 kHz (squares) and 600 kHz (triangles). The error bars for the capacitance and temperature are equal to ±0.01 pF and ±0.1 K, respectively. Ovals and lines were added to help visualize the changes of slope in the curves, which represent transition temperatures.

3. Results

Experimental results for the capacitance C as a function of temperature T are presented in Fig. 1, for CCl_4 confined within MWCNT with $D = 5$ nm. These results were obtained for three different frequencies $\omega = 30$, 100 and 600 kHz, for both closed (pristine) and open-tip (pretreated with CO_2) MWCNT. Our experiments started with a sample at $T = 110$ K, to ensure all the CCl_4 is in solid phase. Only a small change in slope is observed at 250 K for CCl_4 adsorbed on closed MWCNT samples. In contrast, all the curves for CCl_4 adsorbed on open-tip carbon nanotubes exhibit a jump at 234 K and changes of slope at five different temperatures: 172, 205, 225, 250 and 259 K. Bulk CCl_4 melts from a crystalline rhombohedral (Ib) phase to a liquid phase at 250 K, and also undergoes a solid-solid transition between crystalline rhombohedral (Ib) and monoclinic (II) forms at 225 K (Domalski and Hearing, 2003). Both transitions are observed in our experiments as small changes in the slope of the curves, due to the small volume of bulk CCl_4 in the samples. At temperatures higher than 259 K, C scales with $1/T$; this is a clear sign that all the CCl_4 in the system is liquid. MWCNT are representative of porous materials with strongly attractive walls, where the magnitude of the interactions CCl_4-carbon walls is high compared to the CCl_4-CCl_4 interactions. For such systems, experimental and simulation studies have shown that the adsorbate layers near the pore walls are the first to freeze and the last to melt (Radhakrishnan et al., 2002a). In consequence, the maximum observed for all the curves at 259 K should represent the melting of the confined CCl_4 close to the pore walls. We speculate that the feature observed at the lowest temperature (172 K) may correspond to a possible solid-solid transition inside the pore, although further studies are required to confirm this issue. At 205 K there is a slight change of slope in all the curves, suggesting that an inhomogeneous melting process is starting in the confined phase. These changes take place up to 234 K, where there is a sharp increase in C. Since the adsorbate close to the pore walls melts at 259 K, an inhomogeneous confined phase exists at 234 K and consists of liquid CCl_4 in the center of the pore and

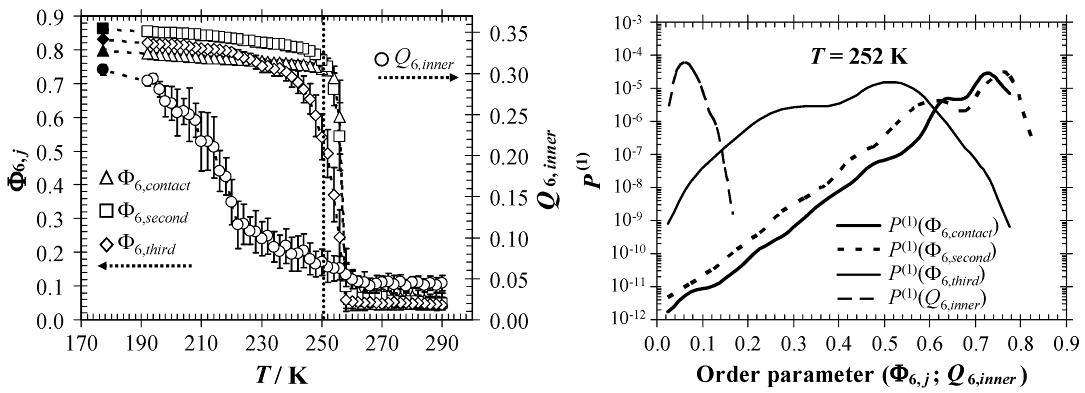

(a) *(b)*

Figure 2. (a) Average values of the bond order parameters measured for LJ CCl_4 confined in a structureless MWCNT with $D = 5$ nm ($D/\sigma_{ff} = 9.7$) and $L = 30.84$ nm ($L/\sigma_{ff} = 60$), as a function of temperature, as obtained from parallel tempering simulations. $\Phi_{6,j}$ was measured for the contact, second and third layers, and $Q_{6,\text{inner}}$ was monitored for the adsorbate in the center of the pore (fourth and innermost layers). The black filled symbols represent results from a GCMC simulation performed at $T = 177$ K. The thick dotted line represents the bulk melting point of LJ CCl_4. (b) First order distribution functions of the probability P (see text for details) for the same system at $T = 252$ K.

solid CCl_4 close to the walls. Further experiments are needed to corroborate our analysis. Direct information about the structure of the confined phase cannot be obtained from dielectric relaxation spectroscopy alone. Experimental techniques such as x-ray diffraction and neutron scattering are suitable to determine the structure of the adsorbed phase. On the other hand, comparisons between experiments and simulations can provide some insight and help in the analysis of the results.

The simulations were performed for LJ CCl_4 adsorbed within a structureless model MWCNT of $D = 5$ nm and $L = 30.84$ nm, for which the confined phase consisted of five layers. In Fig. 2(a) we report the average values of the bond order parameters as a function of temperature, as obtained from grand canonical parallel tempering simulations. The 2-D order parameters $\Phi_{6,j}$ were measured for the three layers close to the walls (contact, second and third), whereas the 3-D order parameter $Q_{6,\text{inner}}$ was determined for the adsorbate in the center of the pore (fourth and innermost layers). The behavior in the contact and second layers is very similar: a steep increase in $\Phi_{6,j}$ around 250–260 K, followed by slight increases in $\Phi_{6,j}$ with further reduction of the temperature. These results suggest that both molecular layers undergo a transition from isotropic liquid to an ordered phase around 250–260 K. This is in good agreement with the experimental results (Fig. 1), where the outer layers melt between 250 and 259 K. In the simulations, the change in $\Phi_{6,j}$ for the third layer is more gradual than for the first two layers and occurs in a wider temperature range, around 220–260 K. The adsorbate in the center of the pore shows gradual increases in $Q_{6,\text{inner}}$ in the range 220–260 K, followed by a quick rise between 220 and 190 K. This is again in agreement with the experiments (Fig. 1), where the features observed between 205 and 234 K can be associated with melting in the inner layers. The behavior of the third layer in the simulations, which is intermediate between the behaviors of the outer and inner regions, is probably masked in the experiments by the features we associate with those regions. The transition observed in the experiments at 172 K was not observed in the simulations.

In order to rigorously determine the thermodynamic stability of the phases, we have used a combination of grand canonical parallel tempering Monte Carlo with the Landau free energy method to sample the probability distribution function of Eq. (3). In Fig. 2(b) we show the first order distribution functions of the probability [e.g., $P^{(1)}(\Phi_{6,\text{contact}})$ was obtained by integrating P with respect to all the order parameters except Φ_6, contact] for the studied system at a representative temperature, $T = 252$ K. In such simulations a wide range of phase space (defined by the combination of the order parameters used) is sampled, as can be seen from Fig. 2(b). There is excellent agreement between the average values of the order parameters at 252 K [Fig. 2(a)] and the values of the order parameters at the global maxima in $P^{(1)}$ [Fig. 2(b)]. The global maxima in each of those functions represent the equilibrium configuration in each layer/region. These free energy calculations provide a rigorous confirmation that the

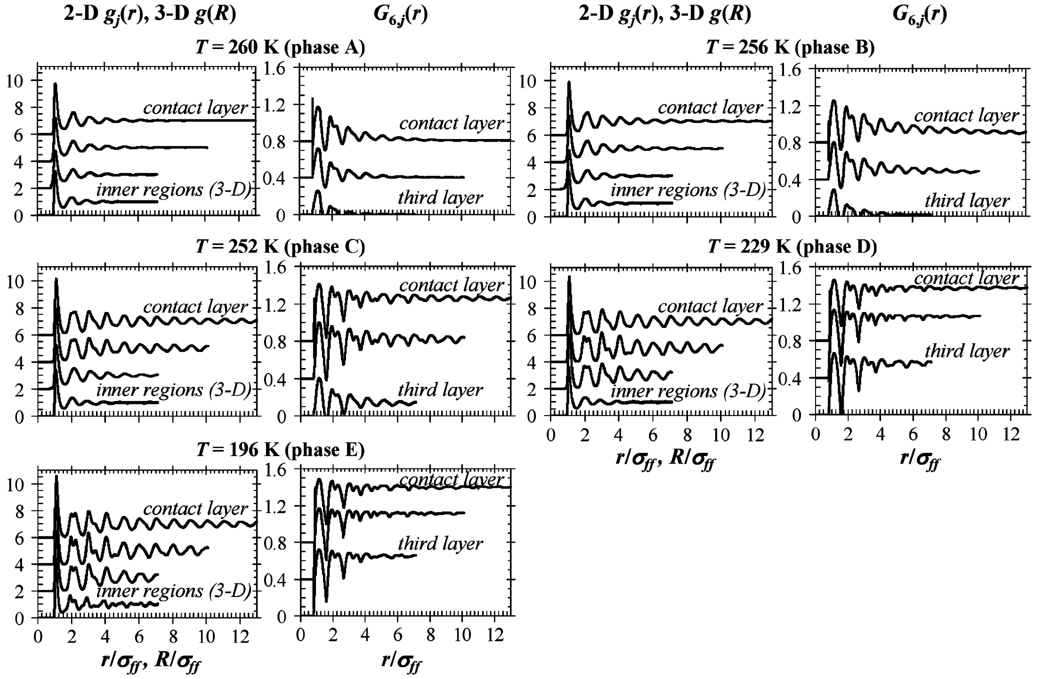

Figure 3. 2-D positional and bond orientational correlation functions, $g_j(\mathrm{r})$ and $G_{6,j}(\mathrm{r})$, for the first three molecular layers of adsorbate, and 3-D positional correlation function corrected by excluded volume effects, $g(R)$, for the adsorbate in the center of the pore. Five different confined phases (see text) can be seen for LJ CCl4 within a structureless MWCNT of $D = 5$ nm ($D/\sigma_{ff} = 9.7$).

results obtained with the parallel tempering technique [Fig. 2(a)] are true equilibrium results.

Results for the 2-D positional and bond orientational pair correlation functions for the first three layers of CCl4 are presented in Fig. 3. We also report the 3-D positional pair correlation function for the inner regions, which has been corrected for excluded volume effects. At $T = 260$ K, the adsorbate exhibits liquid-like features in $g_j(r)$ and $g(R)$, and an exponential decay in $G_{6,j}(r)$ for the first three layers. Therefore, all adsorbate regions behave as dense, liquid-like fluids with short-range positional and bond orientational order (phase A). At $T = 256$ K, the contact and second layers have an intermediate morphology between a 2-D hexagonal crystal and a liquid, while the rest of the adsorbate presents liquid-like structure (phase B). The $g_j(r)$ for the contact and second layers have liquid-like features with extended correlations (as compared to the $g_j(r)$ at 260 K). In addition, the $G_{6,j}(r)$ for these two layers decays at a slower rate (as compared to the $G_{6,j}(r)$ at 260 K); moreover, $\Phi_{6,j}$ for these two layers [Fig. 2(a)] takes intermediate values between those exhibited by a 2-D liquid ($\Phi_{6,j} \sim 0.1$) and a 2-D crystal ($\Phi_{6,j} \sim 0.8$) in our simulations. A rigorous system size scaling analysis, which was done for slit pores to determine the existence of hexatic phases (Radhakrishan et al., 2002b) cannot be performed for the MWCNT studied here ($D = 5$ nm) for large enough sizes, since the dimensions of the quasi-2D layers are limited by pore diameter. In consequence, the intermediate phases observed in the contact and second layers at 256 K cannot be rigorously termed as hexatic phases. Such an analysis can only be performed for cylindrical pores with larger diameters.

At $T = 252$ K, both the contact and second layers appear as 2-D hexagonal crystals with defects, with quasi-long range positional order and long-range bond orientational order. The third layer exhibits an intermediate morphology similar to that observed for the first two layers at 256 K, and the center of the pore keeps its liquid-like characteristics (phase C). The crystalline nature of both contact and second layers is determined from the features observed in the $g_j(r)$ functions: a large value on the first peak, a first minimum of zero and an incipient splitting in the second and third peaks. The constant value of $G_{6,j}(r)$ at relatively large r for the two outer layers is also a signature of ordered hexagonal phases. At $T = 229$ K, the third layer exhibits the same crystalline features as the outer layers, while the inner regions are still liquid-like (phase D). Finally, all

Table 1. Temperature range of stability of each phase for LJ CCl_4 within a structureless MWCNT, $D =$ 5 nm ($D/\sigma_{ff} = 9.7$), $L = 30.84$ nm ($L/\sigma_{ff} = 60$).

Most stable phase	A	B	C	D	E
Range of stability (K)	$T > 257$	$254 < T < 257$	$248 < T < 254$	$214 < T < 248$	$T < 214$

CCl_4 have quasi-crystalline morphology at $T = 196$ K (phase E). The CCl_4 in the inner regions suffers strong geometrical constraints and consists mostly of frustrated crystals with a large number of defects, as is evidenced in the $g(R)$ features. It is important to note that transitions can be observed even in the narrow inner regions, where particles do not exhibit a truly 1-D system behavior (with no phase transitions) because of the interactions with the neighboring molecular layers. Similarly, it has been shown (Radhakrishnan and Gubbins, 1997) that particles forming a 1-D system within a zeolite can undergo gas-liquid phase transitions at low temperatures due to pore-pore correlation effects. Table 1 presents the thermodynamic transition temperatures and the range of stability of each phase, as determined from our free energy calculations. All the transitions were found to be of weakly first order nature.

In summary, results from dielectric relaxation spectroscopy and molecular simulations (including free energy calculations) show evidence of a rich phase behavior for CCl_4 confined within a MWCNT of $D = 5$ nm. Five different phases were found to be stable over extended temperature ranges in our simulations. Multiple transition temperatures above and below the bulk melting point were determined from experiments and simulations, finding consistent agreement between both series of results. In order to gain insights on the effect of pore size and the nature of the pore surfaces, we are currently studying fluids confined within MWCNT and silica pores (Vycor, MCM-41) of different diameters.

Acknowledgments

We are grateful to H. Bock, C. M. Colina (NCSU) and R. Radhakrishnan (UPenn) for helpful discussions, and to F. Beguin and his group (CNRS-Orléans) for synthesizing the MWCNT. This work was supported by the National Science Foundation (CTS-0211792), the Committee of Scientific Research of Poland (KBN 2P03B 014 24), an Adam Mickiewicz University Rector Grant (2003), and a NATO Collaborative Linkage Grant (PST.CLG.978802). Supercomputer time was provided by the National Partnership for Advanced Computational Infrastructure (NSF/NRAC MCA93SO11) and the National Energy Research Scientific Computing Center (DOE DE-FGO2-98ER14847).

References

Delpeux, S., K. Szostak, E. Franckowiak, S. Bonnamy and F. Beguin, “High Yield of Pure Multiwalled Carbon Nanotubes from the Catalytic Decomposition of Acetylene on in-Situ Formed Cobalt Nanoparticles,” *J. Nanosc. Nanotec.*, **2**, 481–484 (2002).

Domalski, E.S. and E.D. Hearing, “Condensed Phase Heat Capacity Data,” *NIST Chemistry WebBook, NIST Standard Reference Database Number 69*, P.J. Linstrom and W.G. Mallard (Eds.), March 2003, National Institute of Standards and Technology, Gaithersburg MD, 20899 (http://webbook.nist.gov).

Gelb, L.D., K.E. Gubbins, R. Radhakrishnan and M. Sliwinska-Bartkowiak, “Phase Separation in Confined Systems,” *Rep. Prog. Phys.*, **62**, 1573–1659 (1999).

Hung, F.R., G. Dudziak, M. Sliwinska-Bartkowiak and K.E. Gubbins, “Freezing/Melting Behaviour within Carbon Nanotubes,” *Mol. Phys.*, **102**, 223–234 (2004).

Morineau, D. and C. Alba-Simionesco, “Liquids in Confined Geometry: How to Connect Changes in the Structure Factor to Modifications of Local Order,” *J. Chem. Phys.*, **118**, 9389–9400 (2003).

Nelson, D.R. and B.I. Halperin,“ Dislocation-Mediated Melting in Two-Dimensions,” *Phys. Rev. B*, **19**, 2457–2484 (1979).

Peterson, B.K., J.P.R.B. Walton and K.E. Gubbins, “Fluid Behaviour in Narrow Pores,” *J. Chem. Soc., Faraday Trans. 2*, **82**, 1789–1800 (1986).

Radhakrishnan, R. and K.E. Gubbins, “Quasi-One-Dimensional Phase Transitions in Nanopores: Pore-Pore Correlation Effects,” *Phys. Rev. Lett.*, **79**, 2847–2850 (1997).

Radhakrishnan, R., K.E. Gubbins and M. Sliwinska-Bartkowiak, “Global Phase Diagrams for Freezing in Porous Media,” *J. Chem. Phys.*, **116**, 1147–1155 (2002a).

Radhakrishnan, R., K.E. Gubbins and M. Sliwinska-Bartkowiak, “Existence of a Hexatic Phase in Porous Media,” *Phys. Rev. Lett.*, **89**, 076101 (2002b).

Radhakrishnan, R. and B.L. Trout, “A New Approach for Studying Nucleation Phenomena Using Molecular Simulations: Application to CO_2 Clathrate Hydrates,” *J. Chem. Phys.*, **117**, 1786–1796 (2002).

Sliwinska-Bartkowiak, M., J. Gras, R. Sikorski, R. Radhakrishnan, L. Gelb and K.E. Gubbins, “Phase Transitions in Pores: Experimental and Simulation Studies of Melting and Freezing,” *Langmuir*, **15**, 6060–6069 (1999).

Steinhardt, P.J., D.R. Nelson and M. Ronchetti, “Bond-Orientational Order in Liquids and Glasses,” *Phys. Rev. B.*, **28**, 784–805 (1983).

Yan, Q. and J.J. de Pablo, “Hyper-Parallel Tempering Monte Carlo: Application to the Lennard-Jones Fluid and the Restricted Primitive Model,” *J. Chem. Phys.*, **111**, 9509–9516 (1999).